Applied Energy 262 (2020) 114403

Contents lists available at ScienceDirect

Applied Energy

journal homepage: www.elsevier.com/locate/apenergy

Agent-based distributed demand response in district heating systems

Hanmin Cai[a], Shi You[a,*], Jianzhong Wu[b]

[a] Department of Electrical Engineering, Technical University of Denmark, 2800 Kgs. Lyngby, Denmark
[b] School of Engineering, Cardiff University, Cardiff CF24 3AA, UK

HIGHLIGHTS

- ADMM-based distributed demand response approach was developed and analysed in detail.
- Buildings jointly optimised heating demands with reduced private information exchange.
- The approach was implemented on microcontrollers and an MQTT-based communication system.

ARTICLE INFO

Keywords:
Distributed demand response
District heating
ADMM

ABSTRACT

Current district heating systems are moving towards 4th generation district heating in which end-users play an active role in system operation. Research has shown that optimising buildings' heating demands can release network congestion and contribute to reducing primary energy usages. Coupled with end-user privacy concerns, an approach in which buildings jointly optimise their heating demands while preserving privacy needs to be investigated. In view of this need, we have developed a distributed demand response approach based on exchange ADMM to support distributed agent-based heating demand optimisation for the district heating system with minimal private information exchanges. This paper summarises mathematical derivation, simulation and implementation of the proposed approach. The results show that the proposed approach obtained the same results as its centralised counterpart proposed in the existing literature and the sensible information exchanges were substantially reduced. An implementation at multiple spatial scales and time scales on micro-controllers and a communication system validates the proposed approach in a practical context. In conclusion, the proposed approach is suitable for real-world implementation in a large-scale district heating system.

1. Introduction

The increasing share of RES generation has induced the need of flexible and integrated energy system operation in order to compensate for the lack of flexibility in RES generation and maintain system stability. As the DH system is moving towards 4th generation DH [1] and is expected to be a crucial part of an integrated energy system, the DHO needs to exploit the flexibility in the system. Throughout this paper, the term flexibility will refer to the capability of deviating from a reference power profile [2]. Among three promising flexibility sources: operational optimisation of generation units [3], thermal inertia of DHN [4], and building heating demand optimisation [5], we have chosen to focus on the role of the heating demand optimisation in system operation to improve quality of service and system efficiency, since the building heating demands take up 40% of the overall energy consumption in Europe [6]. The flexibility can be obtained by balancing between temperature variations and economic/environmental benefits.

The existing DH system operating practices rely on the “critical node“ concept and DHO operates the system according to measurements at the most peripheral substation. This furthest node is denoted as the “critical” node, whereas all other nodes are denoted as the “non-critical“ nodes [7]. The network is assumed to be in a desired status as long as the temperature and pressure at the critical node are within predefined limits [8]. The general operating practice includes: (i) adjusting the supply temperature and the flow rate in the network; and (ii) decreasing the supply temperature until the mass flow cannot be freely varied. Following this strategy, the DH substations passively react to network conditions, and there could be unfair heat distribution in the network when peak demands occur [7]. To put it another way, the nodes closer to the area heat substation extract more heat than the nodes further down the network. As a consequence, the latter suffer from heat deficit and the quality of service is compromised. Moreover,

* Corresponding author.
E-mail addresses: hacai@elektro.dtu.dk (H. Cai), sy@elektro.dtu.dk (S. You), wuj5@cardiff.ac.uk (J. Wu).

https://doi.org/10.1016/j.apenergy.2019.114403
Received 20 August 2019; Received in revised form 2 December 2019; Accepted 14 December 2019
Available online 10 January 2020

Nomenclature

c	cost [DKK]
f	pumping power sensitivity to flow rate [kW·s/kg]
H	scheduling horizon [h]
k	substation performance indicator [kWh/kg]
$\mathbf{L}$	set of pipes [–]
$\dot{m}$	mass flow rate [kg/s]
N	number [–]
p	pressure [kPa]
P	electric power [kW]
t	time step index [h]
W	weighting factor [–]
$\mathbf{Y}$	network incidence matrix [–]
z	auxiliary variable

Abbrevation

ADMM	Alternating Direction Method of Multipliers
CHP	Combined Heat and Power
DHN	District Heating Network
DHW	Domestic Hot Water
DDR	Distributed Demand Response
DR	Demand Response
ICT	Information and Communications Technology
MQTT	Message Queuing Telemetry Transport
RES	Renewable Energy Sources
SCADA	Supervisory Control and Data Acquisition
SH	Space Heating

Greek symbols

λ	dual variable [–]
Δ	difference [–]
ν	iteration number
η	efficiency [–]
γ	weight for penalty term [–]
τ	temperature [°C]
φ	thermal power [kW]
ξ	friction coefficient [kPa·s^2/kg^2]

Subscripts and superscripts

a	ambient
c	critical
cir	circulation loss
cw	cold water
el	electrical
i	building index
q	load node
l	pipe index
max	maximum
min	minimum
n	node
p	pipe
r	return
s	supply

Brange et al. [9] reveal with a comprehensive survey that the congestion problem exists widely and highlight the need for engaging flexible demands in system operation.

Although demand-side flexibility has rarely been considered in the existing DH operating practices, there has been an increasing interest in exploiting flexibility to improve DH system operation. Wernstedt et al. [10] have studied the heating demand reduction potential in a DHN, although the demand shifting potential was not considered. Johansson et al. [11] suggest that heating demands in the DH system can be managed to support CHP's energy arbitrage in the Nordpool electricity market. Foteinaki [12] and Sandersen [13] have investigated how long can heating loads be deferred and demonstrated substantial load shifting potential of SH demand in well-insulated buildings. Our previous work [5] has systematically examined the building heating demand optimisation and the benefits at the district level. Guelpa et al. [14] improve the optimisation of building heating demands via a clustering approach. We have shown in [15] that the electrical system can support the DH system to operate more flexibly and substantially reduce the primary energy usages. However, mentioned works mainly adopt a centralised approach, which requires a significant amount of private information to be transmitted to a central controller. Privacy concern could be one of the barriers for enabling building heating demand optimisation in a large-scale DH system, especially to comply with the regulations [16].

Wemstedt and Davidsson argue that an agent-based approach is appropriate in the DH system, which has a modular, decentralised, changeable, ill-structured, and complex nature [17]. They further state that an agent-based approach is more robust, efficient, flexible, open, scalable and economical than its centralised counterpart. Bünning et al. [18] propose an agent-based approach to integrate distributed heating and cooling sources into the DH system. Even though these works have studied flexible heating demands, a comprehensive overview of flexibility by Vandermeulen et al. [19] has shown that the existing literature lacks advanced distributed strategy in the thermal system. Nonetheless, several distributed approaches based on ADMM can be found in the electrical system. Bahrami and Amini [20] have developed an ADMM-based decentralised energy trading framework, which enables market participants to optimise their schedules jointly. Safdarian et al. [21] propose an ADMM-based approach to reduce energy costs in an electricity distribution system. Their method comprised iterative optimisations at individual household which flattened load profiles asynchronously according to an updated total load profile. Liu et al. [22] develop an ADMM-based algorithm to reduce building electricity costs while satisfying electrical distribution system operating limits. Falsone et al. [23] propose a distributed algorithm to address a resource sharing problem with a time-varying network structure.

Together these studies provide important insights into the building heating demand optimisation in the DH system and the efficacy of ADMM-based approach in supporting the multi-agent deployment. Having said that, the existing literature lacks a distributed mechanism for buildings in the DH system to interact with the DHO to optimise heating demands considering both global hydraulic constraints and privacy preservation. Hence, the aim of this study is to fill this gap and provide a DDR approach based on exchange ADMM [24] to support distributed building heating demand optimisation in DH systems while ensuring global hydraulic constraints are respected with minimal private information exchange. Buildings and DHO are represented by load agents and network agent, respectively.

The original contribution of this study is twofold. First, a comprehensive DDR approach is proposed for buildings to jointly optimise their heating demands considering global network constraints and private information exchanges, in order to support active demand engagement in the 4th generation DH system. Second, the load agents and the network agent are designed and explained in detail to implement the DDR approach at multiple spatial and time scales on distributed microcontrollers and a MQTT-based communication system, which provides insights into how agents interact with each other in real-life DH systems.

The remainder of the paper is organised as follows. Section 2 develops steady-state models for DHN and building heating demands followed by the DDR derivation. Section 3 presents the findings of the research: (i) simulation results validate the convergence of the DDR approach to its centralised counterpart; (ii) implementation validates the effectiveness of the proposed approach. Finally, section 4 gives a brief summary and areas for further research are identified.

2. Methodology

This section first presents steady-state models of a DHN and building heating demands with the parameters of all the models obtained from a real DHN and field measurements. Based on these models, the DDR approach is derived. The methodology adopted in this study can be structured into four parts:

1. modelling of the network and components;
2. formulation of centralised approach to set up the theoretical best case;
3. derivation of the distributed approach applying exchange ADMM;
4. implementation of the proposed approach for validation and assessment.

Moreover, in order to make practical suggestions to industrial applications, we have based all our formulations on the setup of a real DH system in Copenhagen. The real system will be briefly explained before a formulation is provided so as to clarify the implementation presented in Section 3. Nonetheless, we believe the setup is sufficiently representative of both the third generation and the fourth generation DH system, and the methodology proposed in this study can be implemented in other radial urban DH networks.

2.1. DHN model

Fig. 1 provides a conceptual view of an overall DHN that comprises both a transmission network and a distribution network. The former transports heat from CHP far away from residents and the latter extracts heat via area heat substation from the transmission network and distributes heat into individual buildings. This study concerns only the distribution network to which all buildings are attached, and the term DHN refers to the distribution network hereafter. Details about the CHP units and the transmission network can be found in [25]. The steady-state models of the circulating pump, the distribution network and the load nodes are summarised in Eqs. (1)–(4). Note that one load node refers to one DH substation in one building.

The flow distribution in the DHN can be calculated as follows.

$$\boldsymbol{Y}\dot{\boldsymbol{m}}_p = \dot{\boldsymbol{m}}_n \tag{1}$$

where $\boldsymbol{Y} \in \mathbb{R}^{N_\mathrm{p}\times N_\mathrm{p}}$ is the network incidence matrix, $\dot{\boldsymbol{m}}_\mathrm{p} \in \mathbb{R}^{N_\mathrm{p}\times 1}$ and $\dot{\boldsymbol{m}}_\mathrm{n} \in \mathbb{R}^{(N_\mathrm{n}-1)\times 1}$ are the vectors of pipe and nodal mass flow rate, N_p is the total number of pipes ($N_\mathrm{n} = N_\mathrm{p} + 1$), N_n is the total number of nodes, $\boldsymbol{N}_\mathrm{n}$, $\boldsymbol{L}_\mathrm{p}$ and $\boldsymbol{N}_\mathrm{q}$ are the sets of all nodes, all pipes and load nodes respectively.

The pressure drop Δp_l over one pipe is proportional to the square of the mass flow rate inside the pipe $\dot{m}_l$ and can be calculated as follows.

$$\Delta p_l = \xi_l \dot{m}_l^2, \ \forall\, l \in \boldsymbol{L}_\mathrm{p} \tag{2}$$

where ξ_l denotes the friction coefficient of the pipe. The accumulated pressure drop over the circulating pump Δp_pump is the sum of pressure drops from the circulating pump to the critical node in the supply network Δp_s and return network Δp_s, and minimum differential pressure over the critical node Δp_min as in Eq. (3) [7].

$$\Delta p_\mathrm{pump} = \Delta p_\mathrm{s} + \Delta p_\mathrm{r} + \Delta p_\mathrm{min} = 2\sum_{l\in \boldsymbol{L}_\mathrm{c}} \Delta p_{l,\mathrm{s}} + \Delta p_\mathrm{min} \tag{3}$$

where $\boldsymbol{L}_\mathrm{c} \subseteq \boldsymbol{L}_\mathrm{p}$ is the set of pipes in the critical route that links the circulating pump and the critical node. A minimal differential pressure is required to circulate the water at the critical node [26]. An example will be elaborated in section 3 to understand this in a real context.

The electric pumping power P^el_{pump} is calculated using the mass flow rate $\dot{m}_\mathrm{pump}$ at the circulating pump and the pressure drop over the pump Δp_pump. This pumping power is constrained by the capacity of the circulating pump $\bar{P}^\mathrm{el}_\mathrm{pump}$ as follows [7].

$$P^\mathrm{el}_\mathrm{pump} = \frac{\Delta p_\mathrm{pump}\dot{m}_\mathrm{pump}}{\eta_\mathrm{pump}\rho} \leqslant \bar{P}^\mathrm{el}_\mathrm{pump} \tag{4}$$

where η_pump is the conversion efficiency of the circulating pump and ρ is the water density. In practice, Eq. (4) defines the hydraulic bottleneck of the network. Congestion occurs when excessive pumping power is required to circulate the water inside network.

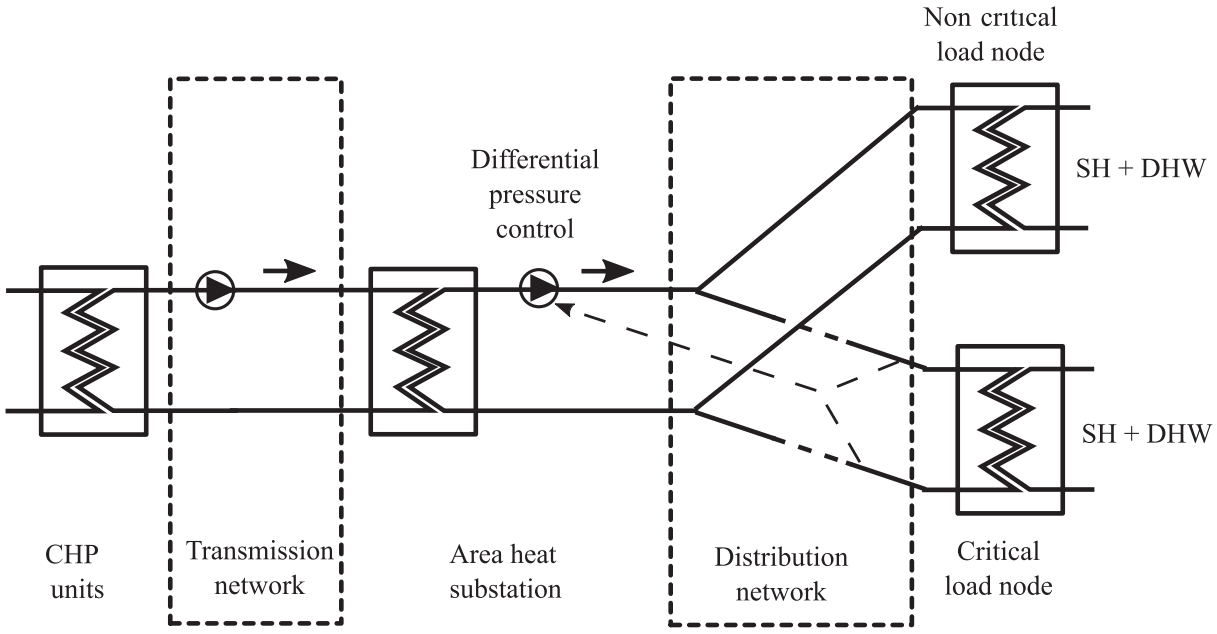

Fig. 1. Schematic diagram of DHN at the transmission and distribution levels.

It can be observed that Eq. (4) is a non-linear global constraint that links all the load nodes. By linearising around operating points, the pumping power $P^{\mathrm{el}}_{\mathrm{pump}}$ can be expressed as a weighted sum of load node mass flow rate $\dot{m}_i$ as follows.

$$P^{\mathrm{el}}_{\mathrm{pump}}(\dot{\boldsymbol{m}}_{\mathrm{q}}) = P^{\mathrm{el}}_{\mathrm{pump}}(\tilde{\dot{\boldsymbol{m}}}_{\mathrm{q}}) + \sum_{i\in \boldsymbol{N}_{\mathrm{q}}} (\dot{m}_i - \tilde{\dot{m}}_i)\frac{\partial P^{\mathrm{el}}_{\mathrm{pump}}}{\partial \dot{m}_i}\bigg|_{\dot{\boldsymbol{m}}_{\mathrm{q}}=\tilde{\dot{\boldsymbol{m}}}_{\mathrm{q}}} \tag{5}$$

where $\tilde{\dot{\boldsymbol{m}}}_q$ is the node mass flow rate vector at the operating points.

Field measurements have shown that temperature drops at the heating substation are relatively stable on an hourly basis [5]. Hence, the DH heating power and node mass flow rate at the service pipe of substation i can be modelled as $\varphi_i = k_i \dot{m}_i$, in which k_i is a time-invariant substation performance indicator and can be interpreted as a constant temperature drop at the load node. In other words, the thermal model of the DH network was neglected in the current study.

In addition, we define $f_i := \frac{\partial P^{\mathrm{el}}_{\mathrm{pump}}}{\partial \dot{m}_i}\Big|_{\dot{\boldsymbol{m}}_{\mathrm{q}}=\tilde{\dot{\boldsymbol{m}}}_q} / k_i$ and $\hat{P}^{\mathrm{el}}_{\mathrm{pump}} := P^{\mathrm{el}}_{\mathrm{pump}}(\dot{\boldsymbol{m}}_{\mathrm{q}}) - P^{\mathrm{el}}_{\mathrm{pump}}(\tilde{\dot{\boldsymbol{m}}}_{\mathrm{q}}) + \sum_{i\in \boldsymbol{N}_{\mathrm{q}}} \tilde{\dot{\boldsymbol{m}}}_i \frac{\partial P^{\mathrm{el}}_{\mathrm{pump}}}{\partial \dot{m}_i}\Big|_{\dot{\boldsymbol{m}}_{\mathrm{q}}=\tilde{\dot{\boldsymbol{m}}}_{\mathrm{q}}}$. Then Eq. (5) can be simplified as Eq. (6).

$$\sum_{i\in \boldsymbol{N}_{\mathrm{q}}} f_i \phi_i = \hat{P}^{\mathrm{el}}_{\mathrm{pump}} \leqslant \bar{\hat{P}}^{\mathrm{el}}_{\mathrm{pump}} \tag{6}$$

where $\bar{\hat{P}}^{\mathrm{el}}_{\mathrm{pump}} = \bar{P}^{\mathrm{el}}_{\mathrm{pump}} - P^{\mathrm{el}}_{\mathrm{pump}}(\tilde{\dot{\boldsymbol{m}}}_{\mathrm{q}}) + \sum_{i\in \boldsymbol{N}_{\mathrm{q}}} \tilde{\dot{m}}_i \frac{\partial P^{\mathrm{el}}_{\mathrm{pump}}}{\partial \dot{m}_i}\Big|_{\dot{\boldsymbol{m}}_{\mathrm{q}}=\tilde{\dot{\boldsymbol{m}}}_{\mathrm{q}}}$. The linearisation above does not aim at an exact calculation of the pumping power. In contrast, it estimates the sensitivity of pumping power's increase to the marginal increase of load node mass flow rate. Hence, by Eqs. (4)–(6), we have turned optimal building heating demands under global hydraulic constraint into an optimal resource sharing problem.

2.2. Building heating demand

Every building in the network has its DH substation supplying the heating demands for both SH and DHW in two separate branches, and only the DHW branch has a water storage tank. To give an illustration, a typical DH substation in a single-family building is depicted in Fig. 2. In such DH substation, an embedded controller (ECL 310) can adjust valve openings and pump speeds to follow an external setpoint [27]. The substation presented here is labelled as level 1. It is the bottom level of a system-wide implementation of the DDR approach. In addition, we assume one agent is responsible for controlling the heating demands of one building.

First-order models were chosen for modelling both SH and DHW demands to develop a system-level strategy in which buildings jointly optimise their heating demands. We have focused on having simple models to estimate the heating demands and facilitate the derivation in the following sections. The parameters were identified from hourly measurements at all DH substations of the entire year of 2017 using a linear regression method [5].

2.2.1. SH model

A first-order SH model is illustrated as an analogy to the electric circuit in Fig. 3 and a lumped building temperature τ^{SH} is assumed to represent one building. Wang et al. [28] argue that the controller built upon detailed in-door climate modelling is strongly affected by the number and placement of sensors. Since this study addresses the coordination of building heating demands optimisation at the system level, we believe first-order models are sufficient to illustrate our methodology, whereas investigating detailed in-door climate modelling of each building based on optimal sensor placement would blur the focus of this study. In the model, thermal conductance C and thermal resistance R of the building envelope, heating power ϕ^{SH}, ambient temperature $\tau^{\mathrm{SH}}_{\mathrm{a}}$ and solar radiation ϕ_{solar} has been considered [5]. After discretising the continuous model presented in Fig. 3 and rearranging, a discrete SH model is presented in Eq. (7). Note that C in Fig. 3 and C^{SH}_i in Eq. (7) refer to different parameters.

$$\tau^{\mathrm{SH}}_{i,t} = A^{\mathrm{SH}}_i \tau^{\mathrm{SH}}_{i,t-1} + B^{\mathrm{SH}}_i \phi^{\mathrm{SH}}_{i,t-1} + C^{\mathrm{SH}}_i \tau^{\mathrm{SH}}_{\mathrm{a},t-1} + D^{\mathrm{SH}}_i \phi_{\mathrm{solar},t-1},\ \forall\, i \in \boldsymbol{N}_{\mathrm{q}} \tag{7}$$

where A^{SH}_i represents the insulation level of building i, B^{SH}_i, C^{SH}_i and D^{SH}_i represent the temperature's sensitivity to the heating power $\phi^{\mathrm{SH}}_{i,t-1}$, the ambient temperature $\tau^{\mathrm{SH}}_{\mathrm{a},t-1}$ and the solar radiation $\phi_{\mathrm{solar},t-1}$, $\tau^{\mathrm{SH}}_{i,t}$ and $\tau^{\mathrm{SH}}_{i,t-1}$ are the lumped building temperatures. In practice, building temperature is regulated by controlling $\phi^{\mathrm{SH}}_{i,t-1}$ according to a weather compensation curve, whereas $\tau^{\mathrm{SH}}_{\mathrm{a},t-1}$ and $\phi_{\mathrm{solar},t-1}$ present external disturbance.

2.2.2. DHW model

The DHW demand was modelled using a bottom-up approach. We combined the water tank characteristics and the stochastic water draw profiles, which were identified from field measurements. Similar to the SH model in Fig. 3, an analogy to electric circuit for DHW is shown in Fig. 4. The discrete DHW model for every building is formulated in Eq. (8).

$$\tau^{\mathrm{DHW}}_{i,t} = A^{\mathrm{DHW}}_i \tau^{\mathrm{DHW}}_{i,t-1} + B^{\mathrm{DHW}}_i \phi^{\mathrm{DHW}}_{i,t-1} + C^{\mathrm{DHW}}_i \tau^{\mathrm{DHW}}_{\mathrm{a},t-1} + D^{\mathrm{DHW}}_i m^{\mathrm{cw}}_{i,t-1},$$
$$\forall\, i \in \boldsymbol{N}_{\mathrm{q}} \tag{8}$$

where A^{DHW}_i represents the water tank insulation level, B^{DHW}_i, C^{DHW}_i and D^{DHW}_i represent the tank water temperature's sensitivity to the heating power $\phi^{\mathrm{DHW}}_{i,t-1}$, the ambient temperature $\tau^{\mathrm{DHW}}_{\mathrm{a},t-1}$ and the water draw $m^{\mathrm{cw}}_{i,t-1}$. In Eq. (8), DH heating power $\phi^{\mathrm{DHW}}_{i,t-1}$ is the only controllable input, the ambient temperature $\tau^{\mathrm{DHW}}_{\mathrm{a},t-1}$ and the water draw $m^{\mathrm{cw}}_{i,t-1}$ represent external disturbances.

2.2.3. SH and DHW flexibility

Flexibility in SH and DHW demands comes from tolerated temperature variations in different physical sources. While DHW usually has a sizeable buffer water tank as shown in Fig. 2, SH relies on building thermal inertia. Literature has shown that minor temperature variations do not have noticeable impacts on human comfort. Moreover, surveys have analysed the economic values of end-users' tolerance on temperature variations. For example, a weekly SH comfort cost profile has

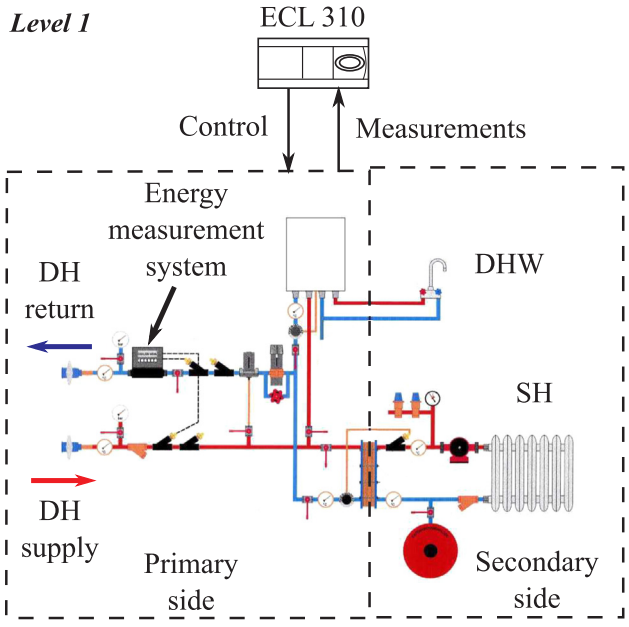

Fig. 2. Illustration of a conventional DH substation in a single-family building [5].

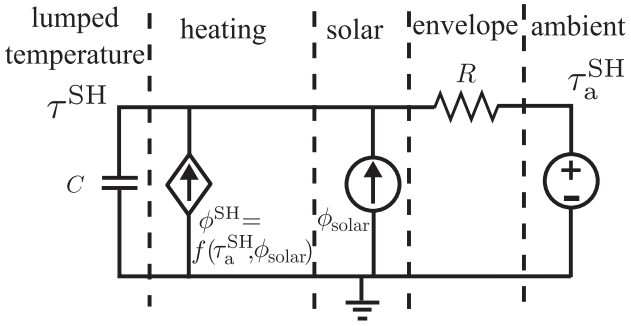

Fig. 3. RC-network of the SH model of one load node.

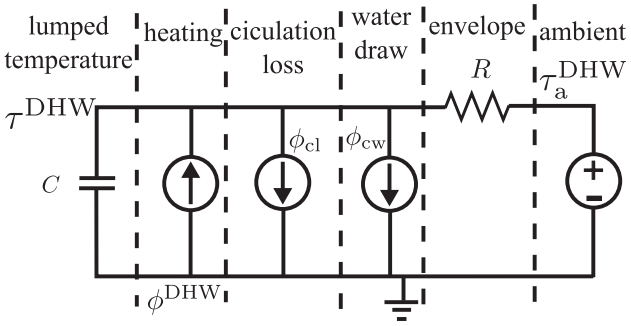

Fig. 4. RC-network of the DHW model of one load node.

been quantified by Chassin et al. [29]. This profile was used in the study to balance between the SH temperature variations and economic gain from modifying heating power. On the other hand, temperature variations in the DHW tank within the predefined temperature zone do not affect the user comfort and the variations need not be associated with a penalty in the objective of the optimisation.

2.3. Building heating demand optimisation

As stated earlier, the existing DH operating practices do not consider DR. Standard DH substation adapts SH heating power according to external temperature using a weather compensation curve, whereas the DHW heating power is controlled according to a fixed DHW temperature setpoint, which is usually 55 °C and occasionally boosted to 60 °C to avoid Legionella contamination. The temperature level is high enough to guarantee a sufficient amount of hot water [30], but also low enough to avoid heating the return pipe. Such standard DH substation is not aware of network condition and heating power is drawn whenever needed. Literature has suggested incorporating an advanced control strategy into the DH substation, such as MPC. It is a recursive optimisation strategy to account for operational constraints and forecast updates. Fig. 5 illustrates its working principle. The energy scheduling of one substation is optimised within the optimisation horizon based on the demand model and local forecasts while respecting the operating constraints. Only the decision for the first time step in the optimisation horizon is executed and the energy schedule is optimised again according to updated weather and user-behaviour forecasts in the next time step. Although MPC with an objective of minimising total energy cost can reduce the cost, concurrent heating demands could occur when there is a universal energy cost profile broadcast to a group of buildings running MPC. That is to say, substations with MPC shift their heating demands into the low price periods and create a load peak in the network [5]. As a result, the quality of service is compromised. This uncoordinated optimisation at the building level in practice counteracts DHO's efforts to improve the quality of service and address congestion in the network. Hence, coordinated building heating demand optimisation needs to be investigated to exploit DR's potential for improving DH system operation fully. The rest of the section is dedicated to deriving DDR and includes two parts. A centralised optimisation of building heating demands, as can be found in existing literature [5], is first formulated. After highlighting the issues with such an approach, the DDR is derived by decomposing the centralised optimisation using exchange ADMM. In other words, the centralised and the distributed approaches solve the same problem with a different control and communication architecture.

2.3.1. Centralised formulation

The underlying assumption of this approach is that one central controller optimises heating schedules of all buildings and coordinate them such that the required pumping power does not exceed the circulating pump's capacity, as formulated in Eq. (4). This requires the measurements and forecasts at every DH substation to be forwarded to the central controller. To ensure the controller adapts to updated forecasts, the receding horizon strategy mentioned earlier is considered in the central controller with an optimisation horizon H. The full formulation is provided in Eq. (9), whose objective balances between energy cost reduction and comfort cost.

$$\underset{\phi_{i,t},\Delta\tau_{i,t}^{SH},z_t}{\text{minimize}} \sum_{i\in\mathcal{N}_q}\sum_{t=1}^{H} c_{1,t}\phi_{i,t} + \sum_{i\in\mathcal{N}_q}\sum_{t=1}^{H} W_{2,i}c_{2,t}(\Delta\tau_{i,t}^{SH})^2 \tag{9a}$$

$$\text{Subject to (7), (8),} \tag{9b}$$

$$\Delta\tau_{i,t}^{SH} = \tau_{i,t}^{SH} - \tau_i^{SH,ref},\ \forall\, t\in H, \forall\, i\in\mathcal{N}_q, \tag{9c}$$

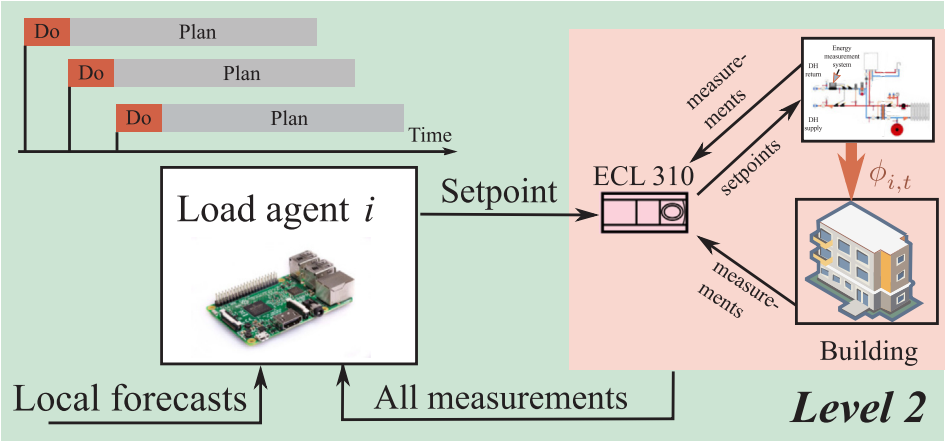

Fig. 5. Illustration of rolling horizon optimisation at one DH substation [31] taking into account measurements from *Level 1* and local weather forecasts.

$$\underline{\tau}_i^{\mathrm{DHW}} \leqslant \tau_{i,t}^{\mathrm{DHW}} \leqslant \bar{\tau}_i^{\mathrm{DHW}},\ \forall\, t \in H,\ \forall\, i \in \boldsymbol{N}_{\mathrm{q}}, \tag{9d}$$

$$0 \leqslant \phi_{i,t}^{\mathrm{SH}} \leqslant \bar{\phi}_i^{\mathrm{SH}},\ \forall\, t \in H,\ \forall\, i \in \boldsymbol{N}_{\mathrm{q}}, \tag{9e}$$

$$0 \leqslant \phi_{i,t}^{\mathrm{DHW}} \leqslant \bar{\phi}_i^{\mathrm{DHW}},\ \forall\, t \in H,\ \forall\, i \in \boldsymbol{N}_{\mathrm{q}}, \tag{9f}$$

$$\phi_{i,t} = \phi_{i,t}^{\mathrm{SH}} + \phi_{i,t}^{\mathrm{DHW}},\ \forall\, t \in H,\ \forall\, i \in \boldsymbol{N}_{\mathrm{q}}, \tag{9g}$$

$$\sum_{i \in \boldsymbol{N}_{\mathrm{q}}} f_i \phi_{i,t} + z_t = \tilde{\bar{P}}_{\mathrm{pump}}^{\mathrm{el}},\ \forall\, t \in H, \forall\, i \in \boldsymbol{N}_{\mathrm{q}}, \tag{9h}$$

$$0 \leqslant z_t,\ \forall\, t \in H \tag{9i}$$

where $W_{2,i}$ is the weighting factor for SH temperature deviations, $c_{1,t}$ is the heating cost profile broadcast by DHO, $c_{2,t}$ is the comfort cost per degree of indoor temperature deviation identified by Chassin et al. [29], $\Delta\tau_{i,t}^{\mathrm{SH}}$ represents SH temperature deviations from the user-defined setpoint $\Delta\tau_i^{\mathrm{SH,ref}}$. $c_{2,t}(\Delta\tau_{i,t}^{\mathrm{SH}})^2$ is included in the objective function to penalise indoor temperature deviation.

Eq. (9c) formulates the temperature deviation from setpoint and the deviation $\Delta\tau_{i,t}^{\mathrm{SH}}$ is included in the cost function Eq. (9a). Eq. (9d) is formulated to bound the DHW temperature within predefined comfort zone. Eqs. (9e) and (9f) formulate the DH power capacity. In Eq. (9g), total heating power is described as a sum of SH and DHW power, as shown in Fig. 2. Note that an auxiliary variable $z_t^{(\nu-1)}$ was added such that Eqs. (9h) and (9i) are mathematically equivalent to the formulation in Eq. (6) and they represent the global hydraulic constraint. Although the heating power $\varphi_{i,t}$ was used in Eq. (9a) instead of energy, they are numerically equivalent since the time step interval is one hour. After solving this centralised optimisation, the energy schedules for every substation $\{\phi_{i,t} | \forall\, i \in \boldsymbol{N}_q, \forall\, t \in H\}$ were obtained and sent to every substation and DH substation executes the power setpoints.

This centralised optimisation approach suffers from three major drawbacks. First of all, the private information exchanges between the DH substation i and the central controller are $\{W_{2,i}, \phi_{\mathrm{solar},t-1}, \tau_{\mathrm{a},t-1}^{\mathrm{SH}}, m_{i,t-1}^{\mathrm{cw}}, \tau_{\mathrm{a},t-1}^{\mathrm{DHW}} | \forall\, t \in H\}$, which include user financial preference $W_{2,i}$; local weather forecasts $\phi_{\mathrm{solar},t-1}$ and $\tau_{\mathrm{a},t-1}^{\mathrm{SH}}$; and user water usage behaviour $m_{i,t-1}^{\mathrm{cw}}$. Since DHO has to collect details of end users' economic preferences and occupancy, privacy concerns could potentially arise. Moreover, the central controller needs to make real-time forecasts of $\phi_{\mathrm{solar},t-1}$ and $\tau_{\mathrm{a},t-1}^{\mathrm{SH}}$ for every DH substation taking into account local condition in order to perform the rolling horizon strategy. This requires tremendous efforts and resources from the DHO. Last but not least, this approach is not modular. From Eq. (9), it can be seen that even one minor change at one DH substation requires the whole optimisation problem to be updated at the central controller. These are issues that need be addressed to realise active demand at a large-scale DH system.

2.3.2. Distributed formulation

From Eq. (9), it can be observed that the problem has a decomposable structure with the complicating constraint Eq. (9h) linking the decision variables of all the buildings in the system, namely DH substation heating power. The centralised formulation in Eq. (9) can be decomposed into one subproblem per load agent using exchange ADMM. Derivation is summarised in Eqs. (10)–(13). First, we define λ_t as the dual variable for Eq. (9h) and the augmented Lagrangian relaxation can be obtained as follows [24].

$$\begin{aligned}\underset{\phi_{i,t},\Delta\tau_{i,t}^{\mathrm{SH}},z_t}{\text{minimize}}\quad & \sum_{i\in\boldsymbol{N}_{\mathrm{q}}}\sum_{t=1}^{H} c_{1,t}\phi_{i,t} + \sum_{i\in\boldsymbol{N}_{\mathrm{q}}}\sum_{t=1}^{H} W_{2,i}c_{2,t}(\Delta\tau_{i,t}^{\mathrm{SH}})^2 + \\ & \sum_{t=1}^{H}\lambda_t(f_i\phi_{i,t} + z_t - \tilde{\bar{P}}_{\mathrm{pump}}^{\mathrm{el}}) + \sum_{t=1}^{H}\frac{\gamma}{2}\left\| \sum_{i\in\boldsymbol{N}_q} f_i\phi_{i,t} + z_t - \tilde{\bar{P}}_{\mathrm{pump}}^{\mathrm{el}} \right\|^2\end{aligned} \tag{10}$$

subject to (9b), (9c), (9d), (9e), (9f), (9g), (9i)

Hence, we can obtain the subproblem for every load agent at iteration ν as in Eq. (11).

$$\begin{aligned}\underset{\phi_{i,t}^{(\nu)},\Delta\tau_{i,t}^{\mathrm{SH}(\nu)}}{\text{minimize}}\quad & \sum_{H}^{t=1} c_{1,t}\phi_{i,t}^{(\nu)} + \sum_{H}^{t=1} W_{2,i}c_{2,t}(\Delta\tau_{i,t}^{\mathrm{SH}(\nu)})^2 + \sum_{H}^{t=1}\lambda_t^{(\nu-1)}f_i\phi_{i,t}^{(\nu)} + \\ & \sum_{H}^{t=1}\frac{\gamma}{2}\left\| f_i\phi_{i,t}^{(\nu)} + \Big(\sum_{i\in\boldsymbol{N}_{\mathrm{q}}} f_i\phi_{i,t}^{(\nu-1)} - f_i\phi_{i,t}^{(\nu-1)}\Big) + z_t^{(\nu-1)} - \tilde{\bar{P}}_{\mathrm{pump}}^{\mathrm{el}} \right\|^2\end{aligned} \tag{11}$$

subject to (9b), (9c), (9d), (9e), (9f), (9g)

where the lumped value $\sum_{i\in\boldsymbol{N}_q} f_i\phi_{i,t}^{(\nu-1)}$, the auxiliary variable $z_t^{(\nu-1)}$ and the dual update $\lambda_t^{(\nu-1)}$ are the information that load agents have received from the network agent at iteration $\nu-1$. One network agent remains necessary to guarantee the global constraint is satisfied. Its problem at iteration ν is formulated as follows.

$$\underset{z_t^{(\nu)}}{\text{minimize}}\quad \sum_{t=1}^{H}\lambda_t^{(\nu-1)}z_t^{(\nu)} + \sum_{t=1}^{H}\frac{\gamma}{2}\left\| \sum_{i\in\boldsymbol{N}_{\mathrm{q}}} f_i\phi_{i,t}^{(\nu)} + z_t^{(\nu)} - \tilde{\bar{P}}_{\mathrm{pump}}^{\mathrm{el}} \right\|^2 \tag{12}$$

subject to $z_t^{(\nu)} \geqslant 0$

The dual update at iteration ν is obtained using the solutions of Eqs. (11) and (12).

$$\lambda_t^{(\nu)} = \lambda_t^{(\nu-1)} + \gamma\Big(\sum_{i\in N_q} f_i\phi_{i,t}^{(\nu)} + z_t^{(\nu)} - \tilde{\bar{P}}_{\mathrm{pump}}^{\mathrm{el}}\Big) \tag{13}$$

To implement Eqs. (11)–(13) in real life, the network agent first broadcasts dynamic price profile $c_{1,t}$ and load agents optimise their

Table 1
Summary of the ADMM-based algorithm, ε denotes the tolerance.

Algorithm

Result: Energy schedules at t
initialization;
while $\nu \leq \nu^{max}$ **do**
  if *residual* $\geq \epsilon$ **then**
    load agents solve Eq. (11) and obtain $\phi_{i,t}^{(\nu)}, \Delta\tau_{i,t}^{\mathrm{SH}(\nu)}$;
    the network agent solves Eq. (12) and obtains $z_t^{(\nu)}$;
    dual update using Eq. (13) to obtain $\lambda_t^{(\nu)}$;
    residual = max{primal residual, dual residual}
  else
    the algorithm converges and exit while loop;
  end
  $\nu = \nu + 1$;
end

energy schedules accordingly by solving Eq. (11). The optimised energy schedules are sent to the network agent, which then solves the optimisation problem formulated in Eq. (12) according to received energy schedules $\varphi_{i,t}^{(\nu)}$ to obtain the auxiliary variable $z_t^{(\nu)}$. With all the information, the dual variable $\lambda_t^{(\nu-1)}$ can be updated and broadcast to all the load agents. An iterative process is required to obtain a solution and the process is further summarised in Table 1. It has been proved in [24] that the results of solving Eqs. (11)–(13) iteratively converge to the optimal solution of the centralised formulation in Eq. (9). Adaptive tuning of γ was applied [32] by balancing between the primal residual and the dual residual. The only information exchanged between load agents and network agent includes only $\lambda_t^{(\nu-1)}$, $\phi_{i,t}^{(\nu)}$ and $\sum_{i\in\mathbf{N}_q} f_i \varphi_{i,t}^{(\nu)}$ at iteration ν.

Although a network agent is still needed to guarantee the network constraints are respected, it does not require detailed knowledge of each building as its centralised counterpart. Compared with the information exchange in the centralised approach, types of information needed to be exchanged are minimised. Local weather forecasts, end-user financial preference and behaviour need not be explicitly exposed. In fact, they can be handled locally to generate only $\varphi_{i,t}$ as shown in Eq. (11). Moreover, every load agent does not receive the energy schedule from any other building, but only the lumped value $\sum_{i\in\mathbf{N}_q} f_i \varphi_{i,t}^{(\nu)}$. Hence we argue that private information exposure is minimised in the DDR approach. Furthermore, the network agent's optimisation problem requires only the information about load agents' energy schedules and does not concern the details of each substation. In other words, the network agent does not need to update its controller if end-users make changes on the substation, such as changing the temperature setpoint etc. This is a significant improvement from the centralised approach as the DDR is more robust to the changes made at the end-user side.

3. Results

3.1. System configuration

A geographical representation of the DHN used in the case studies is shown in Fig. 6 [5]. It is located in Copenhagen's Nordhavn area. The network has a radial structure with 21 residential buildings and 1 commercial building attached to it. It is part of a city-scale DHN with similar building sparsity and network structure. Therefore, the approach proposed in the previous section can be implemented in other parts of the network. A single-pipe diagram further illustrates the network configuration in Fig. 7. A pressure measurement unit is installed at the critical node L17, which is the furthest node from the circulating pump installed at the area heat substation at the beginning of the network. The route connecting the circulating pump and the node L17 is denoted as the "critical" route. The measurements of the critical node are transmitted to DHO's proprietary SCADA system, and the circulating pump is in practice controlled to maintain a minimum differential pressure at node L17 [7] to ensure that water can be circulated through the building.

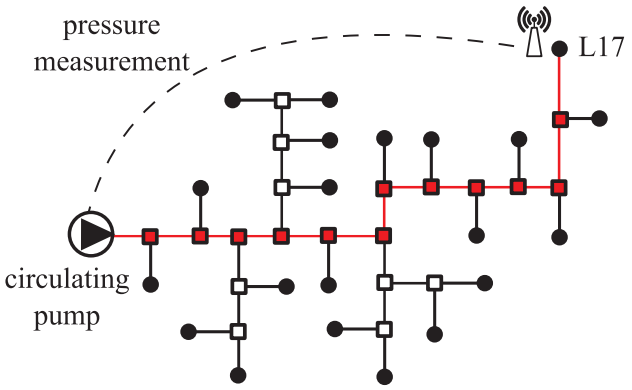

Fig. 7. Nordhavn DHN with the critical route marked in red (each solid circle represents a consumer/load node and each square represents an intermediate node without heating power consumption or injection).

3.2. Case studies

In this section, two case studies are presented. Both of them have been motivated by the procedure of deploying distributed approach in real life, which should generally include three main phases. In the first phase, building heating demands need to be modelled using historical data, and the distributed algorithm needs to be validated in tools such as MATLAB, assuming perfect communication. This provides a deterministic platform and supports fast parameter tuning. In the second phase, the load agents and the network agent implemented on microcontrollers need to be connected via ICT infrastructure since load agents and network agent may be distributed in a wide geographical area. This phase is necessary to evaluate the impacts of communication delays and limited computing power on the feasibility of current technology and most importantly, a low-cost deployment. In the third phase, load agents need to be incorporated into DH substations to assess the economic benefits for the overall system. This section provides two case studies to illustrate phase 1 and 2. More specifically, case 1 verifies whether the DDR obtains the same solution as its centralised counterpart, which is important to eliminate potential errors that could propagate to the next stages. Case 2 examines a pragmatic situation, in which both flexible and inflexible buildings coexist. It also includes multiple spatial and time scales implementation of the DDR approach on microcontrollers and an MQTT-based communication system.

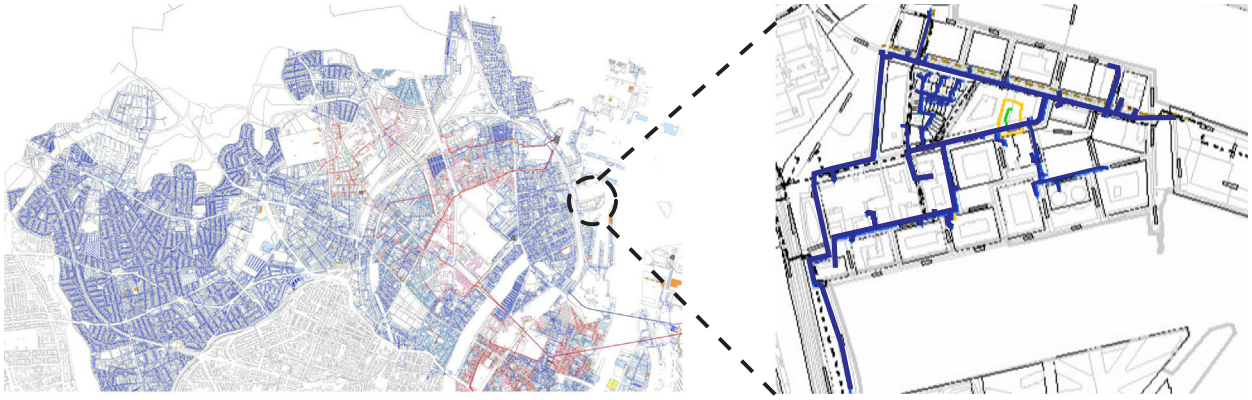

Fig. 6. Nordhavn DHN (right) as part of a city-scale DHN (left).

3.2.1. Case study data

In what follows, we explain in detail how proper data can be obtained to support the real-life implementation. The data required to solve the central optimisation and distributed optimisation problems include: (i) parameters for the DHN; (ii) parameters for building heat demand models; (iii) marginal heat cost; (iv) comfort cost profile; (v) end-user preference; (vi) weather condition; (vii) end-user water draw patterns. The data used in this study were drawn mainly from three sources: DHO [33], Varmelast.dk [34] and Danish standards [30,35]. While the parameters for the DHN can be found in the network design from DHO, the parameters for building heat demand models need to be identified from historical measurements using methods such as linear regression. In this study, the parameters of building SH and DHW demand models have been identified from hourly measurements at all DH substations in the entire year of 2017 using Eqs. (7) and (8) to fit the historical measurements. Although the DH substations measured SH and DHW heating power in an aggregated form, we separated SH and DHW heating power by exploiting the measurements in summer, when SH demand was negligible in the well-insulated buildings in question. The RMSE level of the modelling is presented in Fig. 8 [5]. The modelling errors are mainly attributed to the additional data analysis to separate SH from DHW power. Consequently, calculated SH and DHW power are not exactly the same as the actual values. If they could be measured separately, the modelling errors could be reduced. In the real implementation, this can be compensated by a recursive state-estimation technique such as Kalman Filtering.

As building heating demands were assumed to be flexible to improve system operation, meaningful representation of the benefits from the elastic demand is needed. In the study, the marginal heat production cost in Greater Copenhagen was chosen. One-week marginal cost profile in winter was obtained from the heating market Varmelast.dk and is shown in Fig. 9. It not only indicates the heat production cost at a specific moment but also indicates the CO_2 intensity of each unit of heat energy. This is because CO_2 emissions are penalised, and biomass is subsidised in Copenhagen. Hence, the marginal cost profile in Fig. 9 is positively correlated with the CO_2 content in each unit of heat energy. Optimising heating demands to reduce energy cost can at the same time contributes to CO_2 emission reduction. In addition, such marginal heat cost profile can be obtained from the heat market two days ahead, which represents a suitable time-frame for DHO to broadcast to load agents. While the marginal heat cost profile has real economic and environmental values, end-users' willingness for temperature deviations, namely comfort cost, is rather tangible. It varies during the day and during the week. Hence, the weekly comfort cost profile quantified by Chassin et al. [29] was used to capture this pattern. As for the end-user preferences, SH temperature setpoint of 22 ˚C was assumed. Any temperature variations from this setpoint were associated with a comfort cost. On the other hand, DHW tank temperature was set to be between 45 ˚C and 60 ˚C. 45 ˚C is a suitable temperature level to guarantee sufficient hot water and 60 ˚C is sufficient to avoid Legionella contamination. While weather condition can be obtained from the weather station, end-user water draw patterns should be identified from the historical data. Examples of one residential building and one commercial building are shown in Fig. 10, obtained by averaging the DH power during the summer period. From Fig. 10, we can observe clear daily and weekly patterns, and this motivates us to consider one full week in the case studies. A winter week in 2017, when Fig. 9 was obtained, was chosen, and all the data within that week were used in this case study.

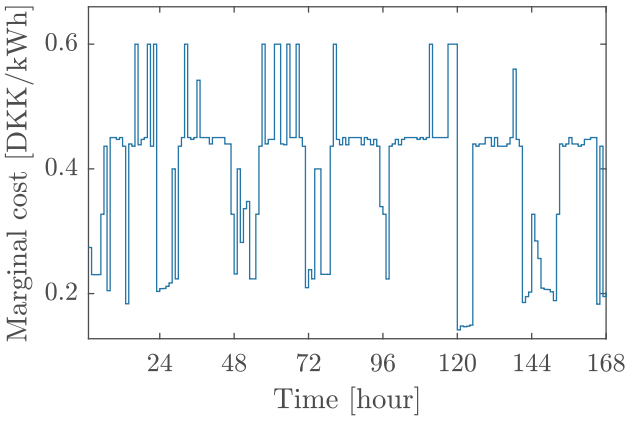

Fig. 9. A typical weekly marginal cost profile of heat production in the Greater Copenhagen in winter [34].

3.2.2. Case 1: simulation

This case study compares the solution obtained from the DDR approach with that from its centralised counterpart in simulation. YALMIP [36] was utilised to formulate the optimisation problem in MATLAB and solver Gurobi was used. It was assumed that the individual substations' actions do not affect the dynamic heat prices. The pumping power capacity $\bar{P}^{el}_{pump}$ was set to be 2.16 kW to limit the concurrent heating demands. The optimisation horizon was set to be 4 h.

Solutions of the centralised approach and the DDR approach are presented in optimization_result_admm_pred4 with respect to SH temperature, DHW temperature, total heating power and circulating pump's pumping power. The solutions for the DDR approach are exactly the same as the centralised approach, and the results overlap with each other in Fig. 11. Hence, we can conclude that with reduced private information exchange, the DDR approach still obtains the same solutions as the centralised approach proposed in the existing literature.

Apart from that, we can observe from Fig. 11 that SH and DHW heating power were effectively shifted toward the low heat price

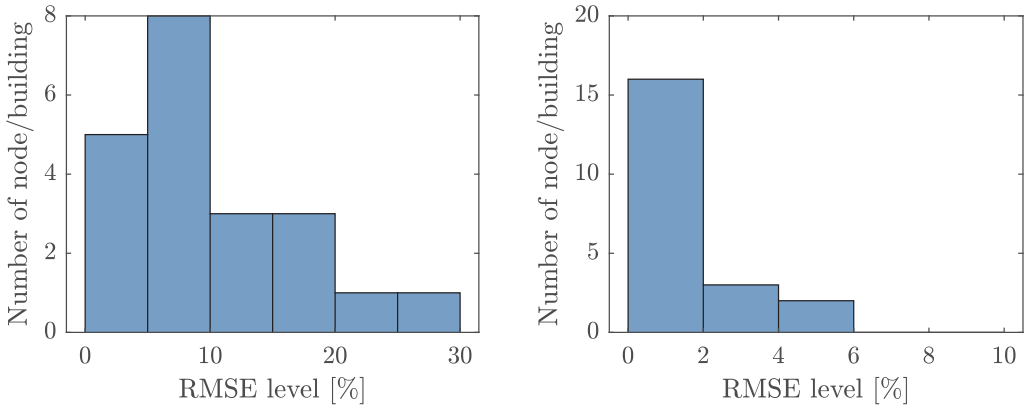

Fig. 8. Histogram of root-mean-square error of SH (left) and DHW (right) model fitting in percentage term.

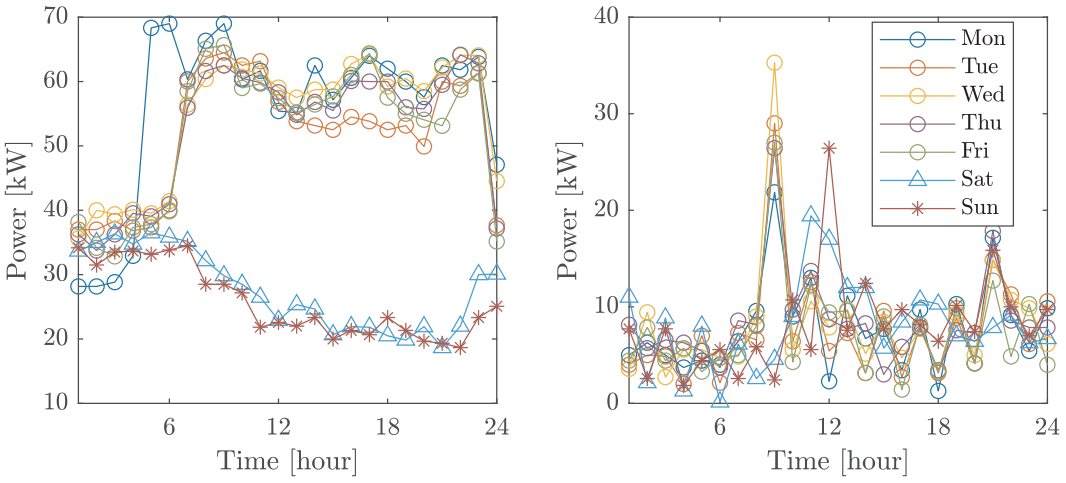

Fig. 10. Illustration of the DHW load daily pattern for one commercial (left) and one residential (right) building over one week.

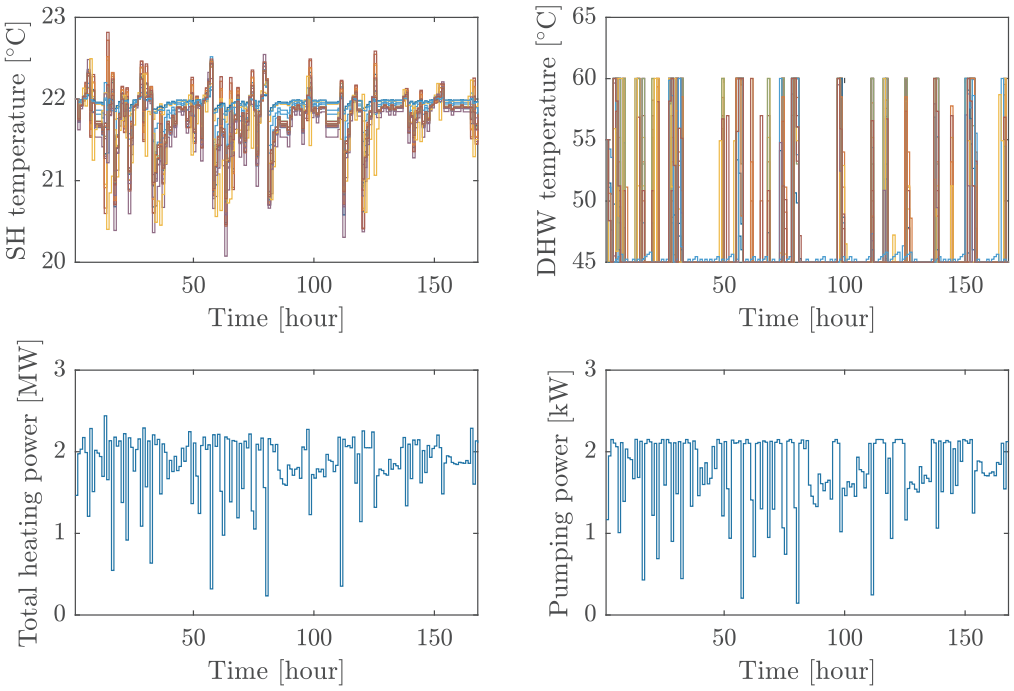

Fig. 11. Results from DDR and centralised approach. Each colour in the top two figures show the SH and DHW temperature of one building.

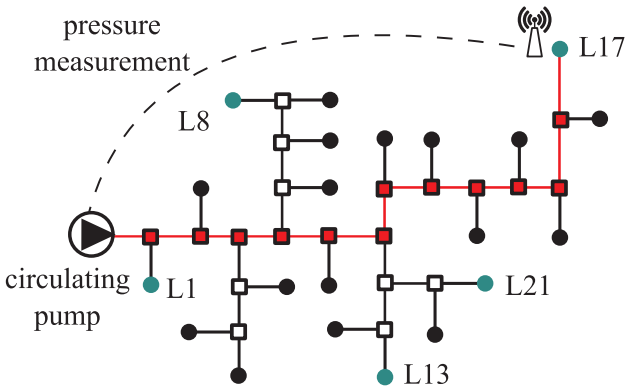

Fig. 12. Coexistence of flexible (green dots) and inflexible (black dots) buildings.

periods. According to the marginal cost profile presented in Fig. 9, the total heating cost in this district is 117.8 kDKK after heating demand optimisation. Whereas under the existing system operational practice, the total energy cost of the district is 123.7 kDKK without any comfort cost because no flexible temperature region is allowed. Hence, coordinated building heating demand optimisation reduces the energy cost by 2.3%. Meanwhile, total comfort cost after heating demand optimisation is 3 kDKK, which is calculated according to the comfort cost profile provided by Chassin et al. [29]. Note that comfort cost is presented here as an indicative compensation for the end-users and calculated as the comfort cost profile multiplied by indoor temperature deviation. A more realistic compensation needs DHO's further economic assessment and business model development taking into account system-wide benefits. Fig. 11 also shows that the circulating pump's pumping power approached to its capacity but did not exceed it, which indicates the global constraint was satisfied.

3.2.3. Case 2: multi-scale implementation

This section presents the concrete designs of the load agent and the

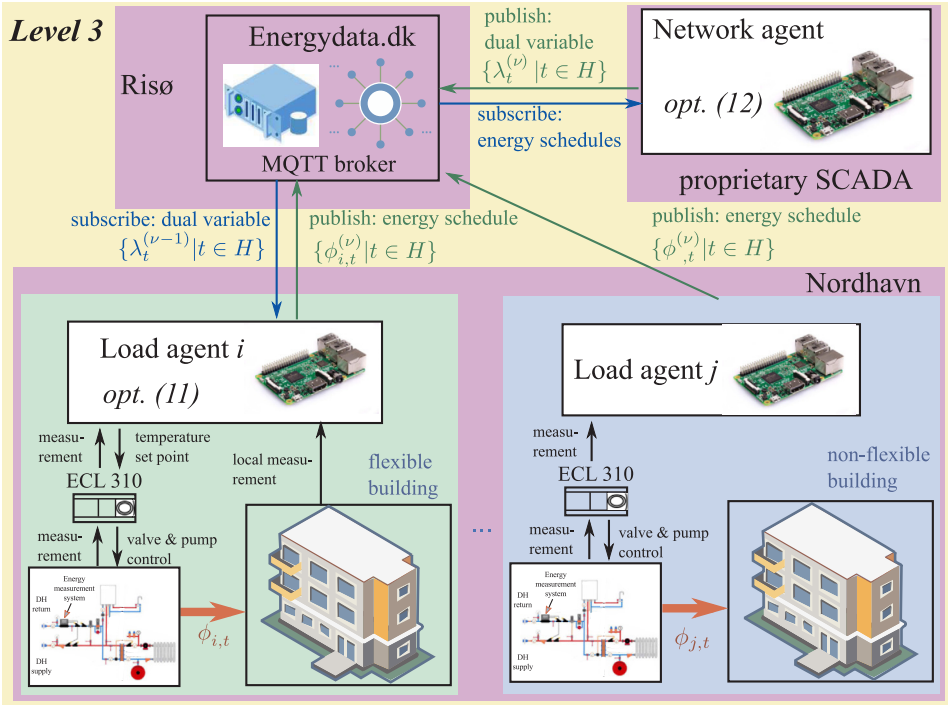

Fig. 13. An overview of the control and communication structure. Note that opt. (11) and opt. (12) in the figure refer to optimisation problems formulated in Eq. (11) and Eq. (12) respectively, and the information flow is not exhaustive.

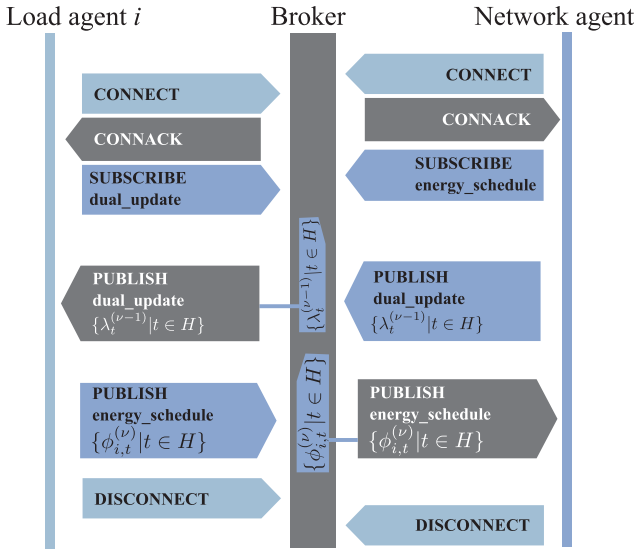

Fig. 14. Illustration of the information flow between the load agent and the network agent based on the MQTT protocol [39].

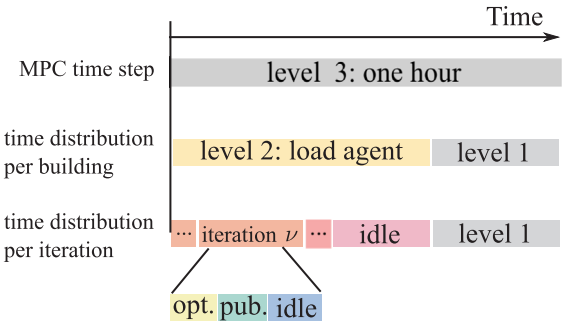

Fig. 15. Illustration of the multiple time scale of the implementation (opt.: optimisation; pub.: publish).

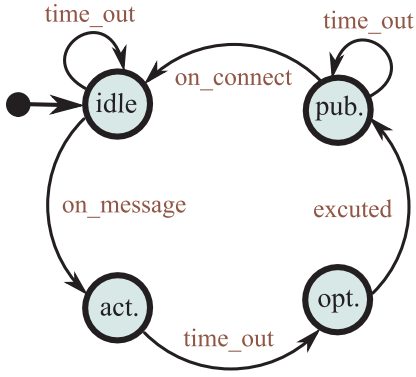

Fig. 16. A finite-state machine for the implementation of the load agents and the network agent (opt.: optimisation; pub.: publish; act.: active).

network agent, which are necessary to implement the DDR approach on microcontrollers. Note that this case study has not physically incorporated the microcontrollers into DH substations. Instead, emulators of buildings based on Eqs. (7) and (8) were used to emulate buildings' response to the optimised energy schedules. In other words, this setup assumes we have perfect modelling of building heating demands. Although emulators with high order models may be constructed, there are two reasons behind our choice. First, emulators with high order models are affected by the number and placement of sensors [28] and are not necessarily give a better representation of the buildings than the first-order model. Second, the assumptions of perfect forecast and modelling are of help to focus on the main topic of this study, which is to validate the efficacy of DDR approach in coordinating building heating demand optimisation. The short-term dynamics are out of the scope of this study.

In addition, this case study examines the situation in which flexible buildings and inflexible buildings coexist, and we show that the DDR approach can incorporate inflexible buildings into the overall approach.

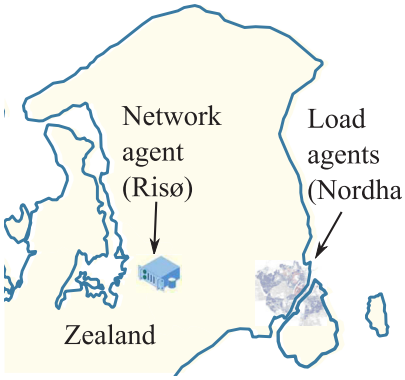

Fig. 17. Illustration of the geographical distribution of the network agent and the load agents.

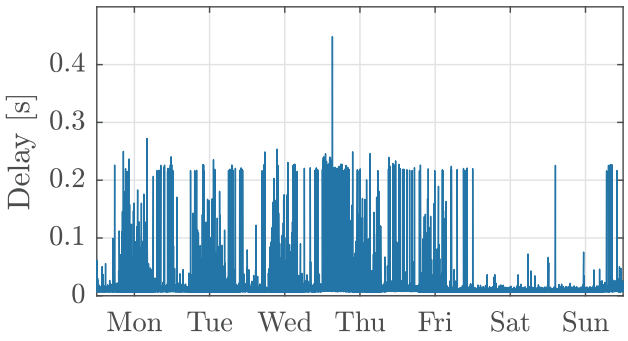

Fig. 19. An identification of the communication delay pattern over one week.

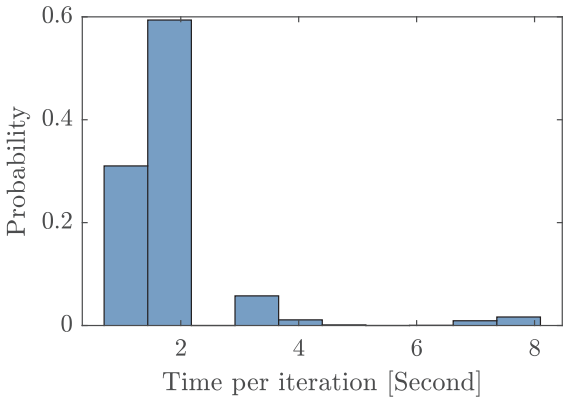

Fig. 20. Normalised histogram of time spent per iteration.

The rationale behind is not only because the system is expected to have a mix of flexible and inflexible buildings depending on end-users' willingness to participate but also the fact that even for flexible buildings, people should be able to freely opt-out and stop optimising their heating schedules. In other words, flexible buildings are responsive to an external signal, whereas inflexible buildings are those that either choose not to participate in system operation or initially participated but chose to withdraw later. While the DDR approach can guarantee the operation to continue without interruption, the centralised approach would require the whole optimisation to be updated. Fig. 12 illustrates the mix of flexible buildings and inflexible buildings.

The overall implementation architecture illustrated in Fig. 13 consists of 5 flexible nodes, 16 inflexible nodes, 1 network agent and the underlying communication flow. The information exchanges and the iterative process have been summarised in Table 1.

The communication system was built based on MQTT protocol [37], which is a lightweight protocol designed for embedded systems with limited computing power and applications in virtual power plant [38]. The protocol adopts a publish/subscribe pattern as illustrated in Fig. 14, which gives an example of exchanging updated energy schedule $\{\varphi_{i,t}^{(\nu)} | \forall\, t \in H\}$ and dual variable $\{\lambda_t^{(\nu-1)} | \forall\, t \in H\}$ between the load agent and the network agent.

The multiple time-scale structure is illustrated in Fig. 15, where level 1, level 2 and level 3 refer to the components depicted in Figs. 2, 5 and 13 respectively. The overall system executes the receding horizon strategy with a time step of one hour, which is denoted as the "MPC time step". The load agents and the network agent then execute the

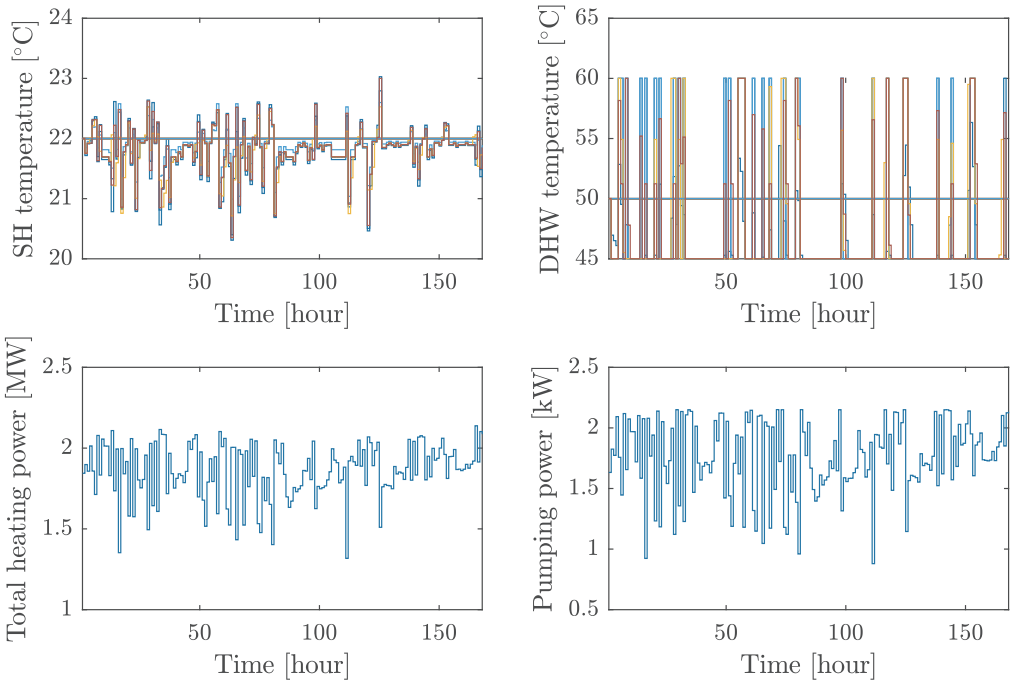

Fig. 18. Results of the joint building heating demand optimisation of distributed the load agents and the network agent implemented on Raspberry Pi. Colours in the top two figures show the SH and DHW temperatures in each building.

DDR's iterative process as summarised in Table 1. In each iteration, the load agents in flexible buildings optimise their heating schedules, publish via the MQTT broker and remain idle until dual variable updates or termination flag from the network agent. Fig. 16 summarises the internal logic of microcontrollers in a finite-state machine. Once the iterative process terminates, the power setpoint for the next time step is forwarded to building emulators, which return building responses.

The multiple spatial scales of the implementation are illustrated in Fig. 17, in which the DDR approach was implemented on microcontrollers distributed around Zealand, an island where Copenhagen is situated. The network agent and the load agents are separated by 30 km. All the load agents were programmed in Python using CVXPY [40] on Raspberry Pi 3 Model B, which features a quad-core 64bit CPU clocked at 1.2 GHz and 1 GB of SDRAM [41]. One purpose of this wide spatial distribution was to assess the extent to which communication and computational delay affect the real-life implementation. Also, DHO may be located far away from the load agents in practice.

The results of load agents' joint optimisation are summarised in Fig. 18, in which the straight lines in the upper half of Fig. 12 show the SH and DHW temperature in the inflexible buildings. The total heating cost and comfort cost of the district were calculated to be 122.1 kDKK and 0.9 kDKK respectively. The results presented in this section validate the overall control and communication architecture; load agents and network agent design.

The round trip communication delays are in summarised Fig. 19. Clear daily and weekly patterns with high delays during working hours can be observed. In addition, we can notice that the round trip communication delays are mostly less than 0.3 s. The duration per iteration is summarised in Fig. 20. It can be observed that the duration per iteration has an average of 1.92 s. Additional communication overheads include the synchronisation between the load agents and the network agent and requests for load agents to resend their schedules upon loss of communication. The average duration per time step was calculated to be 62 s which means the proposed approach can be executed in a timely manner and we conclude that it is suitable for building heating demand optimisation on an hourly basis.

This case study shows that the DDR approach complemented with the detailed design of internal logics has successfully been implemented on microcontrollers, and the MQTT-based communication system supports the implementation of our approach. Although the DDR approach requires less private information to be transmitted at the expense of an iterative process to reach consensus among agents, we have shown that the delays due to the iterative process on the implementation are marginal for hourly heating schedule optimisation.

4. Conclusion

We have shown that in the proposed distributed demand response approach, buildings can jointly optimise heating demands while ensuring global network hydraulic constraint is respected. At the same time, less private information exchange is needed than its centralised counterpart. We have provided a detailed mathematical derivation of the distributed demand response approach followed by a concrete design and implementation on microcontrollers and a MQTT-based communication system. The simulation results show that the distributed demand response approach obtained the same results as the centralised approach proposed in the existing literature; the implementation validated the design of the load agent and the network agent. Furthermore, the privacy preservation and modular feature of the distributed demand response reduce district heating operator's efforts in practical implementation. The distributed demand response approach can be implemented in other networks with the same characteristics as the network in question. Hence, the present findings add to a growing body of literature on exploiting flexible building heating demands, and the study facilitates the active demand involvement in the 4th generation district heating system.

Nonetheless, some limitations need to be noted. The current study assumed that load agents sent their truthful energy schedules. Future work will investigate a mechanism to ensure the truthfulness of load agents' energy scheduling. An implementation at larger scales is necessary to investigate the scalability.

CRediT authorship contribution statement

Hanmin Cai: Conceptualization, Methodology, Software, Validation, Formal analysis, Investigation, Writing - review & editing. **Shi You:** Supervision, Writing - review & editing. **Jianzhong Wu:** Supervision.

Declaration of Competing Interest

The authors declare that they have no known competing financial interests or personal relationships that could have appeared to influence the work reported in this paper.

Acknowledgement

We would like to thank Vladimir Dvorkin, Jalal Kazempour for discussions and Chalampos Ziras for critical review. This research was part of a project which is funded by the Danish EUDP (Energy Technology Development and Demonstration Programme). Project title: EnergyLab Nordhavn - Smart components in integrated energy systems, project number: 64015-0055.

References

[1] Lund H, Werner S, Wiltshire R, Svendsen S, Thorsen JE, Hvelplund F, et al. 4th Generation District Heating (4GDH): integrating smart thermal grids into future sustainable energy systems. Energy 2014;68:1–11.
[2] De Coninck R, Helsen L. Quantification of flexibility in buildings by cost curves–-methodology and application. Appl Energy 2016;162:653–65.
[3] Wang J, You S, Zong Y, Cai H, Holt CT, Dong Z. Investigation of real-time flexibility of combined heat and power plants in district heating applications. Appl Energy 2019;237:196–209.
[4] Li Z, Wu W, Wang J, Zhang B, Zheng T. Transmission-constrained unit commitment considering combined electricity and district heating networks. IEEE Trans Sustain Energy 2016;7(2):480–92.
[5] Cai H, Ziras C, You S, Li R, Honoré K, Bindner HW. Demand side management in urban district heating networks. Appl Energy 2018.
[6] European Parliament. Directive 2010/31/EU of the European Parliament and of the Council of 19 May 2010 on the energy performance of buildings (recast). Off J Eur Union 2010;18(06):2010.
[7] Frederiksen S, Werner S. District heating and cooling. Studentlitteratur 2013.
[8] Grosswindhager S, Voigt A, Kozek M. Predictive control of district heating network using fuzzy DMC. Modelling, identification & control (ICMIC), 2012 proceedings of international conference on, IEEE. 2012. p. 241–6.
[9] Brange L, Lauenburg P, Sernhed K, Thern M. Bottlenecks in district heating networks and how to eliminate them - a simulation and cost study. Energy 2017;137:607–16.
[10] Wernstedt F, Davidsson P, Johansson C. Demand side management in district heating systems. Proceedings of the 6th international joint conference on Autonomous agents and multiagent systems. 2007. p. 272.
[11] Johansson C, Wernstedt F, Davidsson P. 'Combined heat & power generation using smart heat grid. Int Conf Appl Energy; 2012.
[12] Foteinaki K, Li R, Heller A, Rode C. Heating system energy flexibility of low-energy residential buildings. Energy Build 2018;180:95–108.
[13] Sandersen C, Skov M, Honoré K. A manual for how to use existing buildings' heat profiles to improve the design and operation of buildings, tech. rep., HOFOR A/S; 2018.
[14] Guelpa E, Deputato S, Verda V. Thermal request optimization in district heating networks using a clustering approach. Appl Energy 2018;228:608–17.
[15] Cai H, You S, Wang J, Bindner HW, Klyapovskiy S. Technical assessment of electric heat boosters in low-temperature district heating based on combined heat and power analysis. Energy May 2018;150:938–49.
[16] EU, "EU General Data Protection Regulation. < https://eugdpr.org/ > .
[17] Wemstedt F, Davidsson P. An agent-based approach to monitoring and control of district heating systems. International conference on industrial, engineering and other applications of applied intelligent systems. Springer; 2002. p. 801–11.
[18] Bünning F, Wetter M, Fuchs M, Müller D. Bidirectional low temperature district energy systems with agent-based control: performance comparison and operation optimization. Appl Energy 2018;209:502–15.
[19] Vandermeulen A, van der Heijde B, Helsen L. Controlling district heating and

cooling networks to unlock flexibility: a review. Energy 2018;151:103–15.
[20] Bahrami S, Amini MH. A decentralized trading algorithm for an electricity market with generation uncertainty. Appl Energy 2018;218:520–32.
[21] Safdarian A, Fotuhi-Firuzabad M, Lehtonen M. A distributed algorithm for managing residential demand response in smart grids. IEEE Trans Ind Inf 2014;10(4):2385–93.
[22] Liu Y, Yu N, Wang W, Guan X, Xu Z, Dong B, et al. Coordinating the operations of smart buildings in smart grids. Appl Energy 2018;228:2510–25.
[23] Falsone A, Margellos K, Garatti S, Prandini M. Dual decomposition for multi-agent distributed optimization with coupling constraints. Automatica 2017;84:149–58.
[24] Boyd S, Parikh N, Chu E, Peleato B, Eckstein J, et al. Distributed optimization and statistical learning via the alternating direction method of multipliers. Found Trendsin Mach Learn 2011;3(1):1–122.
[25] Ommen T, Markussen WB, Elmegaard B. Lowering district heating temperatures–Impact to system performance in current and future Danish energy scenarios. Energy 2016;94:273–91.
[26] Li H, Svendsen S. Energy and exergy analysis of low temperature district heating network. Energy 2012;45(1):237–46.
[27] Thingvad A. Delivery no.: 4.4d Design, development and testing of low-cost controllers for fuel-shift technologies. tech. rep.. Technical University of Denmark; 2017.
[28] Wang D, Arens E, Webster T, Shi M. How the number and placement of sensors controlling room air distribution systems affect energy use and comfort. International conference for enhanced building operations, (Richardson TX). 2002.
[29] Chassin DP, Stoustrup J, Agathoklis P, Djilali N. A new thermostat for real-time price demand response: cost, comfort and energy impacts of discrete-time control without deadband. Appl Energy 2015;155:816–25.
[30] Dansk Standard, "Norm for vandinstallationer; 2009.
[31] Jones C. Lecture notes for model predictive control ME-425; 2015.
[32] Xu Z, Figueiredo MAT, Goldstein T. Adaptive ADMM with spectral penalty parameter selection. arXiv preprint arXiv:1605.07246; 2016.
[33] HOFOR. < https://www.hofor.dk/ > .
[34] Varmelast. Heating plans. < http://www.varmelast.dk/ > .
[35] DS 469. Danish Standards, Norm for Specification of Thermal Indoor Climate.
[36] Lofberg J. YALMIP: a toolbox for modeling and optimization in MATLAB. In: Computer aided control systems design, 2004 IEEE international symposium on, IEEE; 2004. p. 284–9.
[37] OASIS. < http://mqtt.org/ > .
[38] Lampkin V, Leong WT, Olivera L, Rawat S, Subrahmanyam N, Xiang R, et al. Building smarter planet solutions with mqtt and ibm websphere mq telemetry. IBM Redbooks 2012.
[39] Wikimedia Commons. < https://commons.wikimedia.org/wiki/File:MQTT_protocol_example_without_QoS.svg > .
[40] Diamond S, Boyd S. CVXPY: a Python-embedded modeling language for convex optimization. J Mach Learn Res 2016;17(83):1–5.
[41] Raspberry Pi. Raspberry Pi 3 model B specification. < https://www.raspberrypi.org/ > .